ORIGINAL RESEARCH PAPER

Effect of the addition of Fe3O4 nanoparticles on the performance of polyethersulfone nanofiltration membrane for the rejection of ^{54,56}Mn ions from aqueous solution

Sedigheh Daroumi¹, Mohammad Ali Aroon², Ramin Yavari³,*, Taher Yousefi³, Hosain Ghasemi Mobtaker ³

¹ *Fouman Faculty of Engineering, College of Engineering, University of Tehran, Guilan, Iran*
² *Membrane Research Laboratory, Caspian Faculty of Engineering, College of Engineering, University of Tehran, Tehran, Iran*
³ *Nuclear Fuel Cycle School, Nuclear Science and Technology Research Institute, (NSTRI), Tehran, Iran*

ABSTRACT

In this study, the flat sheet membranes including the neat polyethersulfone (PES) and the mixed matrix membranes (MMMs) containing 20 wt. % polyethersulfone (PES) and various amounts of Fe_3O_4 nanoparticles were prepared using wet phase inversion and conventional casting methods. Manganese ion rejection and permeate flux as a performance evaluation of the prepared membranes were studied and compared. The characteristics of the fabricated membranes and the synthesized nanoparticles were fulfilled by transmission electron microscopy, field emission scanning electron microscopy, and contact angle measurement. The operational parameters such as polymer concentration, pressure, pH, manganese ion concentration, and time for manganese ion rejection and permeability were first optimized on the neat PES membrane. In the next steps, the performance of the fabricated MMMs containing various amounts of Fe_3O_4 nanoparticles and PES (20%wt.) was evaluated and compared under these optimized conditions. Under the optimal conditions obtained for the rejection of manganese, ions by neat PES, the fabricated MMMs had better performance than the neat PES membrane. Also, the results showed that the best performance of the prepared MMMs with the manganese rejection percentage of 89.3% and permeate flux of 28.7 $L.m^{-2}.h$ was found to belong to the PES membranes containing 0.1 wt.% of Fe_3O_4.

Keywords: *Manganese, Fe₃O₄, Mixed Matrix Membranes, Rejection, Nanofiltration*

INTRODUCTION

One of the most important environmental concerns is the contamination of soil, underground, and surface water via wastewater containing heavy metal ions. These metal ions are usually discharged into the environment by the untreated wastewater of various chemical industry activities. Unlike organic contaminants, heavy metals cannot be degraded or destroyed. Hence the presence of these contaminants in the environment and

their accumulation in living organisms can cause destructive effects on the ecology, health of animals, and human beings. Manganese element as one of the important heavy metals has been extensively used in a variety of industries such as ceramics, dry battery cells and electrical, coils, paint, painting materials, glass, match, catalysts manufacturers, galvanized sheets, and especially in the steel production [1]. In addition to the discharge of the untreated wastewater of these industries into the environment, anthropic

activities and the burning of oil and coal are other main source of water pollution by manganese [2]. On the other hand, ^{56}Mn as one of the manganese radioisotopes is formed during normal operation of a nuclear power plant's reactors as a result of the neutron activation of ^{55}Mn in the primary circuits of water reactors. The corrosion of structural material of nuclear power plants such as stainless steel equipment and concrete is the main source of the presence of this element (^{55}Mn) in the reactors cooling water. Also, ^{54}Mn is another radioisotops of manganese which is a versatile radiotracer for use in various applications [3]. Therefore, the presence of these radioisotopes in the environment with the half-lives of $t_{1/2}$=312 d (^{54}Mn), $t_{1/2}$=2.57h (^{56}Mn), and gamma emitters can create risks for biological systems. The recommended safe level for manganese concentration in drinking water by European and developed countries such as the United Kingdom, United States, Japan, and Canada is 50 µg.L^{-1} [4]. The presence of an excess amount of this ion in the water and its entrance into the body of a human being by ingestion can cause diseases such as Parkinson's disease, coronary heart disease, birth defects, impotence in men, insomnia, and alterations in bone formation [5]. Therefore, the removal of even trace amounts of this element and its radioisotopes from wastewater has been of particular interest to scientists around the world. Various techniques such as chemical precipitation, adsorption, biological and contact catalytic oxidation, coagulation/flocculation, membrane filtration, ion exchange, etc. [6-8] have been applied for the removal and separation of manganese ions from wastewater. Among these methods, the nanofiltration process as an intermediate process between reverse osmosis and ultrafiltration is an attractive and effective method for the treatment of effluents. At the same time, this technique benefits from relatively high permeation flux, high rejection efficiency, unique removal capability for divalent ions, low energy consumption, and easy operation [9].

The main core of membrane technology is the membrane material [10]. Polymeric membranes due to their great capabilities in the field of wastewater treatment and the production of different types of asymmetric nanofiltration membranes are most often used in these processes [11]. Some of the most important polymeric materials that are commonly used in the fabrication of membranes are aromatic polyamides (PA), cellulose acetate (CA),

polyvinylidene fluoride (PVDF), polyethersulfone (PES), polysulfone (PSU), and polypropylene (PP) [12]. Among them, polyethersulfone has attracted the attention of many researchers [13] in the removal and separation processes. That is because of its specific properties such as film formation property, good compatibility with hydrophilic additives, thermal and mechanical stability, acceptable chemical resistance to acids and oxidizing substances like fluorine and hydrogen peroxide along with tolerance to a wide range of temperatures and pH, low sensitivity to UV, easy processing, and a broader range of pore sizes [8]. However, the poor inherent antifouling property of this polymeric membrane has limited its application as an efficient membrane in the nanofiltration process [14]. Hence, to overcome this respective shortcoming and enhancement of wettability and performance of PES, a large number of mixed matrix membranes (MMMs) have been extensively synthesized in the last few years [10]. This type of membrane takes advantage of the merits of both polymers and filler materials. In this regard, one of the most effective approaches is the embedding of the hydrophilic nanoparticles in the polymeric matrix [15]. The introduction of nanoparticles into the polymeric membranes not only can improve their antifouling properties but also modify the hydrophilicity, strength, stiffness properties, and water permeability of these polymers [14]. Some of the nanoparticles that have been used in the fabrication of MMMs based on polyethersulfone are; graphene oxide, functionalized multiwalled carbon nanotubes, activated carbon, zinc oxide, iron oxide, tin oxide, aluminum oxide, titanium oxide, cerium oxide, copper oxide, and so on [16-18]. The super hydrophilic character of Fe_3O_4 nanoparticles makes them promising toward large quantities of OH functional group attachments. Therefore, the incorporation of Fe_3O_4 nanoparticles can appreciably improve the hydrophilicity of the PES membrane, thereby enhancing the water permeability and resistance of antifouling while treating manganese ions (19). Also, these nanoparticles can adsorb metal ions and increase their rejection from aqueous solution in the membrane process. Nevertheless, a review of the kinds of literature indicates that no studies have been yet done on the removal of manganese by MMMs containing PES and Fe_3O_4 nanoparticles. Therefore, this study aims to fabricate MMMs by introducing Fe_3O_4 nanoparticles into PES and

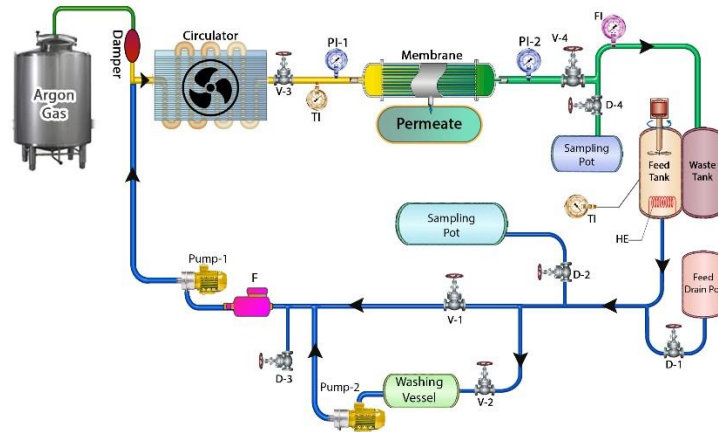*J. Water Environ. Nanotechnol., 9(1): 44-54 Winter 2024*

45

Fig. 1. Schematic depiction of nanofiltration setup

investigating their ability of them in the reject of manganese ions from aqueous solution.

Experimental

Materials

Manganese chloride, N-methyl pyrrolidone (NMP), polyvinylpyrrolidone (PVP), Fe_3O_4, and other chemicals and reagents were obtained from E. Merck or Fluka companies. Polyethersulfone with a molecular weight of 58000 was provided from BASF SE, Germany.

Synthesis of Fe_3O_4 nanoparticles

The synthesis of Fe_3O_4 nanoparticles in the solution phase was carried out as follows [20]. 2.22g of Iron(III) chloride and 0.866 g of Iron(II) chloride were dissolved in 40 ml of demineralized water. While the temperature was gradually increased up to 70 °C under nitrogen atmosphere and refluxing conditions, the solution was stirred at 1000 rpm. After 20 min, a specific value of ammonia solution (0.5 M) was added and then the mixture was stirred for 30 min. Afterward, 2 mL of citric acid solution (2.6 mM) was added to the mixture. The temperature of this mixture was gradually raised to 90 °C while the mixture was stirred and refluxed. Finally, after cooling the mixture, the black Fe_3O_4 nanoparticles were filtered, washed five times with demineralized water, and dried in an oven at 50 °C for 48 hours.

Membrane Fabrication

The flat sheet membranes including neat PES and PES/Fe_3O_4 were fabricated by wet phase inversion and conventional casting methods.

To do this, at first, the determined amount of neat polyethersulfone was mixed with N-methyl pyrrolidone as a solvent. After an additional 0.25 wt. % polyvinylpyrrolidone, this mixture was sonicated for 30 min and stirred for 24 h to distribute and solve entirely these particles in NMP. Also, to prepare the MMMs, the various amounts of prepared Fe_3O_4 were added to NMP and homogenized by ultrasonic bath. After that, PVP and PES were added and dispersed. The air bubbles into these polymeric solutions were omitted using an ultrasonic bath for 30 min and allowed to settle overnight. To prepare flat sheet membranes, these mixtures were cast on a glass plate with a casting knife with a thickness of 100μm and immediately they were immersed in a demineralized water bath. The prepared polymeric films were kept in demineralized water for 24 hours. Finally, these membranes were dried at 25 °C for 24h [21].

Membrane porosity and mean pore size

The overall membrane porosity (ε) can be calculated by Eq. (1) as follows:

$$\varepsilon(\%) = \left(\frac{W_w - W_d}{\rho_f V_m} \right) \times 100 \tag{1}$$

where W_d, W_w, V_m, and ρ_f are the weight of the dried membrane (g), the weight of the wet membrane (g), membrane volume (cm³), and water density (g.cm⁻³), respectively. The experiments were carried out three times for each sample to minimize the experimental errors.

The Guerout–Elford–Ferry equation (Eq. (2)) was also applied to estimate the mean pore sizes of prepared membranes by using pure water flux and porosity [22].

46

J. Water Environ. Nanotechnol., 9(1): 44-54 Winter 2024

$$r_m = \sqrt{\frac{(2.9 - 1.75_\varepsilon)8\eta LQ}{\varepsilon A \Delta p}} \qquad (2$$

where η, Q, ΔP, L, A, and ε are the water viscosity (8.9×10^{-4} Pas), permeated water flow rate ($m^3.s^{-1}$), operating pressure (1 Mpas), membrane thickness (80×10^{-6} m), membrane area

(33×10^{-4} m^2) and the porosity, respectively.

Equipment

Field emission scanning electron microscopy (FESEM) model S-4160, Hitachi (Japan) was used to characterize the morphology of the synthesized nanoparticles and flat sheet membranes. Transmission electron microscopy (TEM) micrographs were obtained with a transmission electron microscope (CM30, Phillips) using the acceleration voltage of 200 kV. The sessile drop method using a contact angle measurement instrument (OCA15EC, Data Physics, Germany) was utilized to measure the static contact angle. Optical microscope images were immediately captured for subsequent contact angle measurement. Inductively coupled plasma-optical emission spectroscopy (ICP-OES) technique was used to the amount of manganese ions. To evaluate the performance of the fabricated neat PES and MMMs for manganese ions rejection, a cross-flow stainless steel nanofiltration (NF) setup was selected (Fig. 1). As shown in Fig. 1, the NF setup is outfitted with a membrane cell with an effective area of 33 cm^2. The operating pressure of both sides of the cell was monitored by two pressure gauges (Wika, Korea). In addition, a high-pressure dosing pump (Jesco, Germany) was used to transfer the feed solution into the membrane cell. Other main constituents used on the NF setup were two flow meters on permeate and retentate streams, one pressure control valve, and one pressure safety valve.

RESULTS AND DISCUSSION

FESEM and TEM images were utilized to study the structure and morphology of the fabricated flat sheet membranes and nanoparticles. Fig. 1 shows a TEM image of Fe_3O_4 nanoparticles which proves the nanometric structure of these prepared nanoparticles. Also, as can be seen in Fig. 2, iron oxide particles are relatively spherical and their size is less than 30 nm.

Cross-section and top surface SEM images of mixed matrix membranes and the neat PES

have been presented in Fig. 3. As can be seen in Fig. 3a, the relatively thin and dense active skin layer has formed the top surface of all fabricated membranes which plays the key role in the rejection of ions in the solution. Also, the typical porous and similar asymmetric structures with this active skin layer supported by the fully developed finger-like cavities and macroporous sublayer can be seen in fabricated flat sheet membranes. This observed structure is typical for PES membranes manufactured using N-methyl pyrrolidone as a solvent and DMW as a coagulation batch [23]. Also, these images show that with addition of Fe_3O_4 doesn't change the asymmetric structure of these membranes. As can be seen in Fig. 3, by increasing these nanoparticles in the casting solution, in addition to the relative increase in thicker active layer, the finger-like structures of these fabricated MMMs became longer, straight, and wider compared to the nest PES (Fig. 3b). With addition of nanoparticles, the casting solution viscosity is increased and it could result in the delayed exchange of NMP and DMW as a solvent and non-solvent, respectively [18]. This phenomenon led to the formation of a less porous membrane, a relatively smaller number of finger-like macro voids with denser and thicker skin layers [24].

The membrane surface hydrophilicity property is one of the important parameters that can influence permeate flux and antifouling ability of the membranes. As proved in previous studies, higher hydrophilicity properties of the membranes will lead to higher permeation flux and a lower tendency toward biofouling, too [23]. Therefore, the water contact angle measurement as a common method was used to characterize the hydrophobicity of the prepared membrane
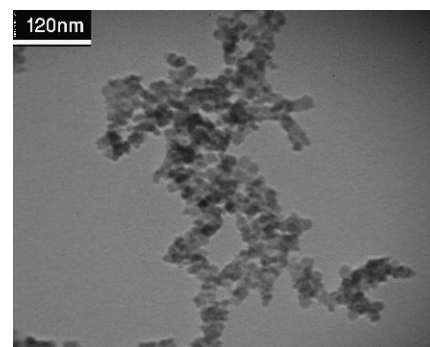

Fig. 2. TEM image of the prepared Fe_3O_4 nanomaterial

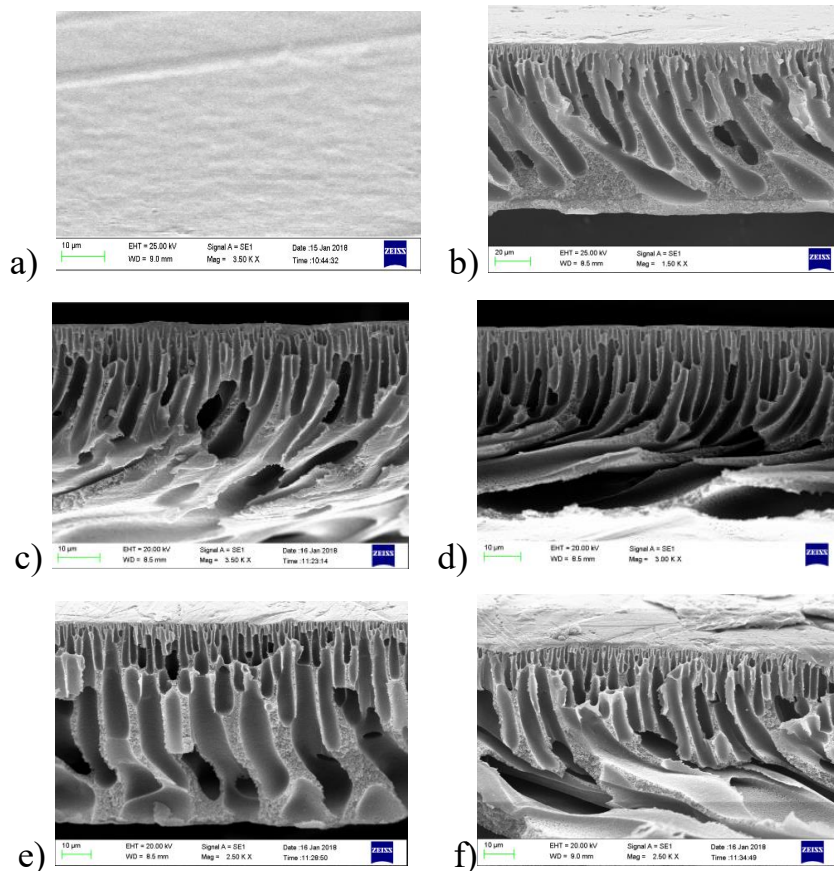*J. Water Environ. Nanotechnol., 9(1): 44-54 Winter 2024*

47

Fig. 3. Top surface (a) and Cross section FESEM images of PES (20%) (b) and MMMs containing PES membrane (20 wt.%) and various concentrations of Fe$_3$O$_4$, c) 0.05 wt.%, d) 0.1 wt.%, e) 0.2 wt.%, f) 0.5 wt.%.

Table 1. The contact angels of the fabricated membranes

No.	samples	Contact angel				
		0.0 (%)	0.05 (%)	0.1 (%)	0.2 (%)	0.5 (%)
2	Fe$_3$O$_4$/PES	68.18 ± 0.13°	64.84 ± 0.29°	63.89± 0.18°	61.91± 0.19°	60.75 ±0.23°

surfaces. Table 1 summarizes the obtained results of the water contact angle at three random locations for the fabricated membranes to minimize the experimental error. As can be seen in Table 1, the amount of contact angles was reduced after the incorporation of Fe$_3$O$_4$ into the neat PES membrane structure. A lower contact angle indicates that the fabricated mixed matrix membrane should have a more hydrophilic surface and better wettability to water which results in higher water flux and antifouling properties.

Table 2 presents the porosity and mean pore size of prepared neat PES and Mixed matrix membrane. As can be seen, the porosity and mean pore size for the fabricated mixed matrix membranes are higher and larger, respectively, compared to the neat PES membrane. This can be assigned to increase of phase inversion rate mainly by utilizing hydrophilic Fe$_3$O$_4$ nanoparticles in the casting solution. In addition, the possible interactions between nanoparticles and polymer binder can reduce the interactions between polymer-polymer chains which leads to the production of large micro-voids [25]. The decrease of porosity and pore size of nanocomposite membrane at a high additive ratio may be attributed to the increase of casting solution viscosity which reduces the mass exchange rate [26].

48

J. Water Environ. Nanotechnol., 9(1): 44-54 Winter 2024

Table 2. The porosity and mean pore size of all prepared membrane

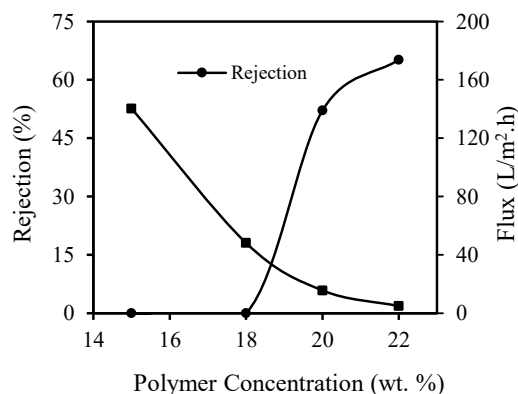| No.	Membrane	Porosity (%)	Mean pore size (nm)
1	Neat PES	74.37	1.23
2	PES + 0.05 %wt. Fe_3O_4	78.42	2.32
3	PES + 0.1 %wt. Fe_3O_4	78.71	2.47
4	PES + 0.2 wt.% Fe_3O_4	87.25	2.84
5	PES + 0.5 wt.% Fe_3O_4	89.80	2.95

Fig. 4. Manganese ion rejection percentage and permeate flux by the flat sheet membrane comprising neat PES versus polymer concentration.
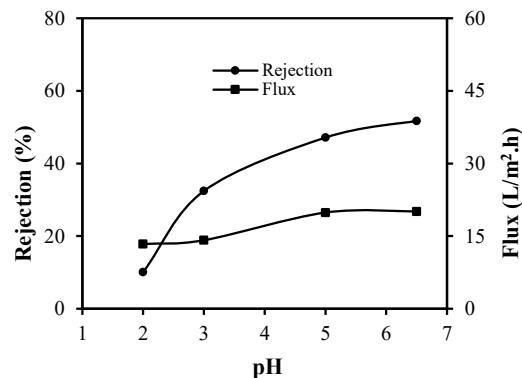

Fig. 5. Manganese ion rejection percentage and permeate flux by the flat sheet membrane comprising neat PES versus the pH of the feed solution.

Permeate flux and manganese ion rejection experiments

Permeation tests including permeate flux and the amount of manganese ion rejection were performed to evaluate the efficiency of the prepared polyethersulfone membranes and its mixed matrix membranes. For this purpose, the operational conditions were firstly optimized for the rejection of manganese ions using the flat sheet membrane of the neat PES, and after that, the rejection behavior of the mixed matrix membranes was investigated and compared in the obtained optimum conditions.

Fig. 4 shows the manganese ion rejection percentage and the amount of permeate flux as a function of PES concentration. The used membranes were fabricated by wet phase inversion and conventional casting method using the preparation of four solutions containing 15, 18, 20, and 22 wt.% PES in NMP as a solvent. As shown in Fig. 4, with increasing PES concentration in casting solution, the rejection percentage of manganese ion is increased while permeate flux is decreased. This can be explained by increasing the casting solution viscosity as a result of the rise in the concentration of polymer. Consequently, the rate of the solvent transfer into the non-solvent and the rate of the non-solvent into the polymer will

be decreased which leads to a lower porosity and a lower permeability of the membrane [27]. At the same time, decreasing the size of the membrane pore results in I) the rise in sieving property of the prepared flat sheet membrane and consequently, the rise in the manganese ion rejection and II) the decrease in the value of solvent passing through the membrane and thus, the deduction of the amount of permeate flux or permeability [28]. To test and evaluate the membrane's performance, an optimal concentration of polymer should be selected, therefore an appropriate permeate flux should be combined with a good rejection of manganese ions. The results show that the rejection of manganese ions increases with the rise of polymer concentration. Accordingly, the highest possible concentration of polymer would be advantageous for this rejection, but it is disadvantageous for the value of permeation flux. The optimal concentration was fixed as 20 wt.% polyethersulfone. In the following of this research work, all the membranes made with this concentration will be studied.

Another important factor that can influence the membrane surface charge and the type of metal species is the solution pH. Therefore, this factor can affect the rejection properties and the amount of permeate flux [29]. For this reason, the pH of the
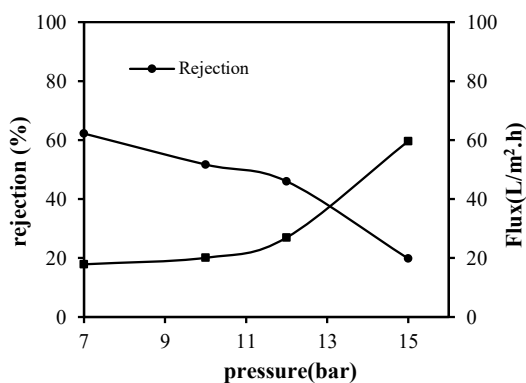
Fig. 6. Manganese ion rejection percentage and permeate flux by the flat sheet membrane comprising neat PES versus pressure.
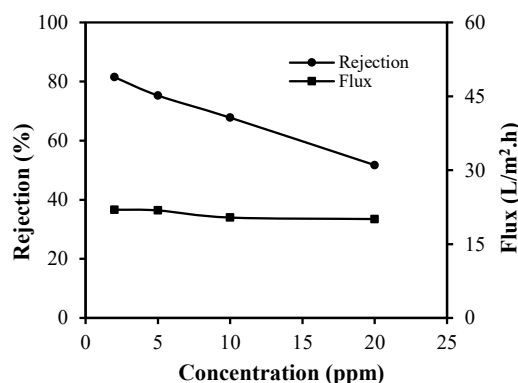

Fig. 7. Manganese ion rejection percentage and permeate flux by the flat sheet membrane comprising neat PES versus initial concentration of manganese ion.

solution is usually the key factor for controlling the rejection process [30]. The relationship of permeate flux and manganese rejection percentage with the solution pH is illustrated in Fig. 5. Based on the solubility product of $Mg(OH)_2$ ($pK_{sp}=11$), the predominant species of manganese ion at pH values above 7 is $Mg(OH)_2$. Therefore, these experiments were performed up to 6.5. As shown in Fig. 5, both rejection percentage and permeate flux increase with a rise in the amount of the solution pH. It is well known that the negative surface charge of the PES membrane originates from the functional groups of PES (O=S=O) [21]. A higher solution pH value results in an increment in the negative surface charge of the PES membrane which leads to stronger electrostatic charge repulsion between the anion in the solution (chloride ion) and membrane surface. This increases the rejection of chloride ions and consequently, the rejection of manganese ions increases due to the Donnan effect [31]. On the other hand, at low pH where the hydronium ion concentration is high, a progressive neutralization of negative sites of the PES membrane surface takes place and the negative surface charge of the membrane reduces. Therefore, chloride ions can easily pass through the membrane and following that, to maintain the charge balance of the solution, manganese ion crosses the membrane [9]. Also, the increase of membrane permeability at higher pH may be due to the expansion of the cross-linked-membrane polymer network and the highest net driving force due to the lowest osmotic pressure at the membrane surface as a result of the reduction of concentration polarization effect [31].

Information on the effect of pressure on the rejection of manganese ions and permeate flux was

obtained by variation of the operating pressure in the range of 7 to 15. The results are shown in Fig. 6. As can be seen, the increase in the operating pressure results in an increase in permeate flux. This increase could be due to the enhancement of driven force (pressure) and adsorption of water on the membrane surface which leads to the increment of solvent passage through the membrane [32]. Moreover, as shown in Fig. 6, manganese ion rejection declines with the rise in the operating pressure. This phenomenon could be explained by the fact that the increasing pressure will cause more manganese ion transports and aggregates on the surface of the PES membrane through convective transport. Therefore, the concentration polarization will increase and result in a decrease in manganese ion rejection by decreasing the charge effect [33].

Fig. 7 presents the curve illustrating the efficiency of manganese ion rejection and permeate flux by the neat PES membranes studied in terms of the initial concentration of manganese ions in the solution. The operating pressure was held constant at 10 bar. As can be seen from this figure, an increase in manganese ion concentration leads to the decline of manganese ion rejection and permeate flux. The decline of permeate flux and the rejection of manganese ion with the increasing of the feed solution concentration can be explained as follows:

I) As the concentration increases, the concentration polarization effect becomes more obvious and weakens the electrostatic forces between the membrane and the ions in the solution which finally results in the passing of manganese ions through the membrane and decreases its
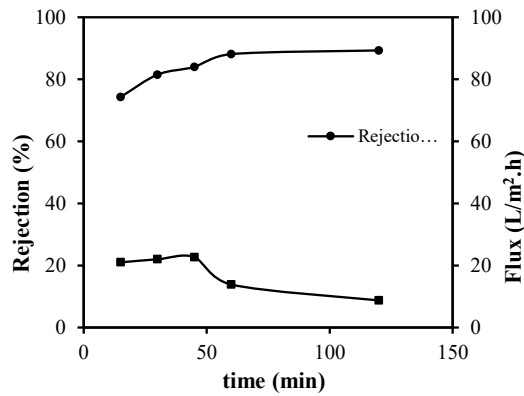
Fig. 8. Manganese ion rejection percentage and permeate flux by the flat sheet membrane comprising neat PES versus time.
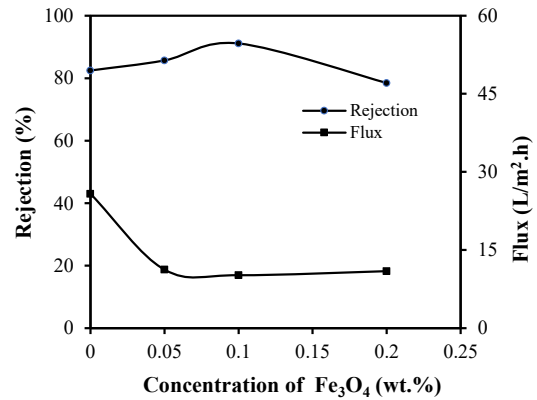

Fig. 9. Manganese ions rejection percentage and permeate flux by the flat sheet MMMs comprising neat PES (20 wt.%) and Fe_3O_4 versus various amounts of Fe_3O_4

Table 3. The performance comparison of the prepared membranes

membrane	Parameter	Percentage of nanoparticle			
		0 wt.%	0.05 wt.%	0.1 wt.%	0.2 wt.%
PES/Fe₃O₄	Rejection percentage (%)	82.5	85.7	91.13	84.47
	Permeate flux (L/m²h)	25.8	11.25	10.17	10.95

rejection [29, 32].

II) the increase of manganese ion concentration in the feed solution enhances osmotic pressure which leads to the decline of permeate flux and thus the rejection decrease due to the decrease of solvent passing through the membrane [9].

To evaluate the performance stability of the flat sheet membrane of PES, long-term tests were performed. Fig. 8 shows permeate flux and manganese ion rejection behavior versus time.

As shown in Fig. 8, with elapsing the experimental time (after 45 min), the amount of permeate flux declined. This behavior can be due to the effect of various factors such as the formation of concentration polarization and pores clogging as a result of ion aggregation on the surface of the membrane [34] that hinder the solvent from passing through the membrane and increase manganese ion rejection, too.

The influence of Fe_3O_4 content on manganese ion rejection percentage and permeate flux was studied. The obtained results have been shown in Fig. 9 and indicate that the rejection percentage of manganese ion was enhanced with a rise in the amount of Fe_3O_4 in the PES membrane up to 0.1 wt.%. The reason for that is the homogeneous distribution of Fe_3O_4 nanoparticles throughout the PES membrane which can form a dense top layer

and improve the rejection percentage of manganese ions [15]. Moreover, by adding and well dispersion of these nanoparticles in PES membrane (up to 0.1 %wt.) and consequently increment of available active sites and higher surface area of nanoparticles, manganese ion rejection percentage increases because of the inherent properties of adsorption of nanoparticles [35]. At higher nanoparticle concentrations (>0.1 %Wt.), the possibility of nanoparticles agglomeration reduces the water flux. In addition, pores filling/blockage would decrease the size of membrane channels which decline the water flux [36]. The higher nanoparticle percentage in MMMs decreased salt rejection slightly. Decrease of manganese ion rejection for MMMs with 0.2 %wt. nanoparticles is assigned to its high porosity and larger pore size which make possible the salt percolation through the membrane.

In this test, the best efficiency was found in MMMs containing PES/Fe₃O₄ (0.1 wt.%). Despite the increment of the hydrophilicity properties of MMMs containing PES and Fe_3O_4 nanoparticles (Table 1), permeate flux is associated with a decrease and this can be due to the increase in the viscosity of the casting solution by adding Fe_3O_4 concentration. As mentioned before, this decreases the rate of NMP as a solvent into the demineralized water (non-solvent) and the rate of the non-solvent

J. Water Environ. Nanotechnol., 9(1): 44-54 Winter 2024

51

Table 4. Summary of some research reports investigated manganese removal by membrane processes

Membrane	Feed solution	Initial manganese concentration (mg·L^{-1})	Removal efficiency (%)	Comments	Ref.
PES/Fe₃O₄	Simulated solution	2	91.13	pH=7, Pressure = 10 bar, Permeation flux = 10.17 Lm².h,	-
NF270	Simulated solution	0.5	85	pH=1.5, Pressure = 4 bar, Permeation flux = 22.5 Lm².h	33
Microfiltration (MF) Polymeric polyether sulfone (SUPOR200)	Artificial and natural groundwater	2	85	Oxidation as pre-treatment pH = 8, Feed temperature = 8 ◦C, Pressure = 8.4 kPa, Permeation rate = 0.5 m h^{-1}	37
Microfiltration (MF) ZeeWeed (ZW-150)	Raw groundwater	1.5	98	Design flux = 51 Lm^{-2}h^{-1} in winter (T = 2 ◦C) Design flux = 68 Lm^{-2}h^{-1} in summer (T = 20 ◦C)	38
Microfiltration (MF) Poly-tetra-fluoro-ethylene	Raw groundwater	0.5	97	Chlorine oxidation as pre-treatment Pressure = 120 kPa Power consumption = 0.2–0.3 kW m^{-3}, Microbial removal rate = 99.99 %, Residual manganese decreased to <0.01 mg·L^{-1} after 2 weeks of operation.	39
Ultrafiltration (UF) polyether sulfone (PES) and polyvinylidene fluoride (PVDV)	Groundwater	1.71-2.28	95	Air oxidation as pre-treatment pH = 6.8–7.3, Feed temperature = 5–8 ◦C, Feed turbidity = 1.13–2.95 NTU, Pressure = 70 mbar	40
Ultrafiltration (UF) Polyvinyl chloride (PVC)	Simulated groundwater	1	90	Aeration and sand filter as pre-treatment pH = 6.75 Feed turbidity ≤ 1 NTU The formation of manganese oxides reduces the membrane fouling. Manganese sand-coated films increase the redox potential of water.	41
Nanofiltration (NF) Polyethersulfone	Natural groundwater	0.36	90	Temperature = 10 ± 1 ◦C Cross flow velocity = 0.12 ± 0.01 m s$\square$1 Pressure = 5–8 bar Membrane effective area = 0.1750 m$\square$2 Compared to NF270 and NF92 membranes, HFNF offered a higher productivity. The hardness of GW negatively impacts the charge exclusion.	42

into the polymer which leads to a smaller porosity and a lower value of permeate flux [28].

Performance comparison

Table 3 shows the performance of the prepared MMMs (PES/Fe₃O₄) along with the neat polyethersulfone membrane. As can be seen, the rejection percentage of the prepared MMMs is higher than the neat PES membrane which indicates an increase in the performance of these membranes as a result of increasing these nanoparticles. Also, this table shows that the permeate flux amount of MMMs has decreased as compared with the neat PES membrane. Despite the increase in hydrophilicity properties of the membranes as a result of the increase of these nanoparticles, the amount of permeate flux in MMMs is reduced. This can be described concerning the mutual effect

of these nanoparticles on membrane porosity increment against reduction of mean pore size which decreases the membrane flux (Table 2).

To compare a summary of some research reports investigated for manganese removal by membrane processes has been presented in Table 4.

CONCLUSIONS

In this study, wet phase inversion and conventional casting methods were used to prepare the nanofiltration membranes of the neat PES and MMMs. The hydrophilicity properties of the neat PES and the rejection performance of manganese ions were improved using Fe_3O_4 nanomaterials. The best performance of the neat PES was achieved at 20 wt.% PES, pressure 10 bar, lower concentration of manganese ions, and pH=6.5. The investigation of MMMs performance prepared by the addition of nanomaterials in the structure of PES indicates that under similar operational conditions, the rejection percentage of manganese ions has significantly been improved, while their permeability of them was declined. The best performance of the fabricated membranes was found to belong to MMMs containing PES membranes (20%) and Fe_3O_4 (0.1 wt.%). Therefore, we can conclude that this prepared membrane can used for the removal of manganese and its radioisotopes (^{54}Mn, ^{56}Mn) from aqueous solution and nuclear wastewater, too.

CONFLICT OF INTEREST

The authors hereby declare that there is no conflict of interest.

REFERENCES

1. He D, Shu J, Wang R, Chen M, Wang R, Gao, Y, Liu R, Liu Z, Tan D, Gu H, Wang N (2021) A critical review on approaches for electrolytic manganese residue treatment and disposal technology: Reduction, pretreatment, and reuse. J Haz Mat. 418: 126235. https://doi.org/10.1016/j.jhazmat.2021.126235.

2. Rudi NN, Muhamad MS, Chuan LT, Alipal J, Omar S, Hamidon N, Hamid NHA, Sunar NM, Ali R, Harun H (2020) Evolution of adsorption process for manganese removal in water via agricultural waste adsorbents. Heliyon. 6:050049. https://doi.org/10.1016/j.heliyon.2020.e05049.

3. Mehboob K, Al-Zahrani YA, Ajohani MS, Alhawsawi A (2021) Primary coolant activity of ^{54}Mn, ^{59}Fe, ^{58}Co, ^{60}Co, and ^{51}Cr in system integrated small and modular reactor. Ann. Nucl. Ene. 160:108356. https://doi.org/10.1016/j.anucene.2021.108356.

4. Iyare PU (2019) The effects of manganese exposure from drinking water on school-age children: A systematic review. Neu. Toxic. 73:1-7. https://doi.org/10.1016/j.neuro.2019.02.013

5. Ahmadi-Asoori S, Tazikeh-Lemeski E, Mirabi A, Babanezhad E, Habibi Juybari M (2021) Preparation of nanocellulose modified with dithizone for separation, extraction and determination of trace amounts of manganese ions in industrial wastewater samples. Microchem J. 160:105737. https://doi.org/10.1016/j.microc.2020.105737.

6. Yang H, Yan Z. Du X, Bai L, Yu H, Ding A, Li G, Liang H, Aminabhavi TM (2020) Removal of manganese from groundwater in the ripened sand filtration: biological oxidation versus chemical auto-catalytic oxidation. Chem Eng J. 2020, 382:123033, https://doi.org/10.1016/j.cej.2019.123033

7. Cheng Y, Xiong W, Huang T (2020) Removal of manganese from groundwater in the ripened sand filtration: biological oxidation versus chemical auto-catalytic oxidation. Sci Total Environ. 737:139525, https://doi.org/10.1016/j.scitotenv.2020.139525.

8. Patil DS, Chavan SM, Oubagaranadin JUK (2016) A review of technologies for manganese removal from wastewaters. J Environ Chem Eng. 4:468. https://doi.org/10.1016/j.jece.2015.11.028.

9. Murthy ZVP, Chaudhari LB (2008) Application of nanofiltration for the rejection of nickel ions from aqueous solutions and estimation of membrane transport parameters. J Haz Mat. 160:70-77, https://doi.org/10.1016/j.jhazmat.2008.02.085.

10. Shu L, Xie LH, Meng Y, Liu T, Zhao C, Li JR (2020) A thin and high loading two-dimensional MOF nanosheet based mixed-matrix membrane for high permeance nanofiltration. J Mem Sci. 603:118049, https://doi.org/10.1016/j.memsci.2020.118049

11. Naddeo V, Banat F, Hasan SW (2020) Preparation of novel polyvinylidene fluoride (PVDF)-Tin(IV) oxide (SnO_2) ion exchange mixed matrix membranes for the removal of heavy metals from aqueous solutions. Sep Pur Tech. 250:117250, https://doi.org/10.1016/j.seppur.2020.117250

12. Giwa A, Ahmed M, Hasan SW (2019) Polymeric Materials for Clean Water. Springer.

13. Balkanloo PG, Mohmoudian M, Hosseinzadeh MT (2020) A comparative study between MMT-Fe_3O_4/PES, MMT-HBE/PES, and MMT acid activated/PES mixed matrix membranes. Chem Eng J. 396:125188, https://doi.org/10.1016/j.cej.2020.125188.

14. Vatanpour V, Madaeni SS, Khataee AL, Salehi E, Zinadini S, Monfared HA (2012) TiO_2 embedded mixed matrix PES nanocomposite membranes: Influence of different sizes and types of nanoparticles on antifouling and performance. Desalination. 292:19-29, https://doi.org/10.1016/j.desal.2012.02.006

15. Jamil TS, Mansor E, Abdallah H, Shaban AM, Souaya ER (2018) Novel anti fouling mixed matrix CeO_2/Ce_7O_{12} nanofiltration membranes for heavy metal uptake. J Environ Chem Eng. 6:3273-3282, https://doi.org/10.1016/j.jece.2018.05.006.

16. Giwa A, Hasan SW (2020) Novel polyethersulfone-functionalized graphene oxide (PES-fGO) mixed matrix membranes for wastewater treatment. Sep Pur Tec. 241:116735, https://doi.org/10.1016/j.seppur.2020.116735.

17. Parani S, Oluwafemi OS (2020) Fabrication of superhydrophobic polyethersulfone-ZnO rods composite Membrane. Mat Let. 281:128663, https://doi.org/10.1016/j.matlet.2020.128663.

18. Khorshidi B, Hosseini SA, Ma G, McGregor M (2019)

J. Water Environ. Nanotechnol., 9(1): 44-54 Winter 2024

53

Novel nanocomposite polyethersulfone- antimony tin oxide membrane with enhanced thermal, electrical and antifouling properties. Polymer. 163, 48-56. [https://doi:10.1016/j.polymer.2018.12.058]

19. Al-Husaini IS, Mohd Yusoff AR, Lau WJ, Ismail AF, Al-Abri MZ, Wirzal MZH (2019) Iron oxide nanoparticles incorporated polyethersulfone electrospun nanofibrous membranes for effective oil removal, Chem Eng Res Des. 148: 142–154, https://doi.org/10.1016/j.cherd.2019.06.006

20. Nigam S, Barick KC, Bahadur D (2011) Development of citrate-stabilized Fe_3O_4 nanoparticles: Conjugation and release of doxorubicin for therapeutic applications. J Magn Magn Mater. 323:237-243, https://doi.org/10.1016/j.jmmm.2010.09.009.

21. Vatanpour V, Esmaeili M, Davood Abadi Farahani MH (2014) Fouling reduction and retention increment of polyethersulfone nano filtration membranes embedded by amine-functionalized multi-walled carbon nanotubes. J Memb Sci. 466:70-81, https://doi.org/10.1016/j.memsci.2014.04.031

22. A. Bagheripour E, Moghadassi AR, Hosseini SM, Van der Bruggen B, Parvizian F (2018) Novel composite graphene oxide/chitosan nanoplates incorporated into PES based nanofiltration membrane: chromium removal and antifouling enhancement. J Ind Eng Chem, 62:311–320 https://doi.org/10.1016/j.jiec.2018.01.009

23. Goncukov Z, Rezanka J, Dolina J, Dvorak L (2021) Sulfonated polyethersulfone membrane doped with ZnO-APTES nanoparticles with antimicrobial properties. Reac Funct Poly. 162:104872, https://doi.org/10.1016/j.reactfunctpolym.2021.104872.

24. Hosseini SA, Soltanieh M, Mousavi SM (2017) Investigating morphology and performance of cellulose acetate butyrate electrospun nanofiber membranes for tomato industry wastewater treatment. Desalin Water Treat. 64:127-135, https://doi.org/10.5004/dwt.2017.20141.

25. Baghbanzadeh M, Rana D, Matsuura T, Lan CQ (2015) Effects of hydrophilic CuO nanoparticles on properties and performance of PVDF VMD membranes. Desalination 369:75–84. https://doi.org/10.1016/j.desal.2015.04.032.

26. Hosseini SM, Madaeni SS, Khodabakhshi AR (2012) The electrochemical characterization of ion exchange membranes in different electrolytic environments: investigation of concentration and pH effects. Sep Sci Technol 47: 455–462. https://doi.org/10.1080/01496395.2011.615046

27. Ismail AF, Goh PS, Sanip SM, Aziz M (2009) Transport and separation properties of carbon nanotube-mixed matrix membrane. Sep Puri Tech. 70:12-26, https://doi.org/10.1016/j.seppur.2009.09.002.

28. Nouri AR, Yavari R, Aroon MA, Yousefi T (2019) Multiwalled Carbon Nanotubes/Polyethersulfone Mixed Matrix Nanofiltration Membrane for the removal of cobalt ion. J Water Environ Nanotech. 4:97-108, https://doi.org/10.22090/jwent.2019.02.002.

29. Ghasemi Torkabad M, Keshtkar AR, Safdari SJ (2017) Comparison of polyethersulfone and polyamide nanofiltration membranes for uranium removal from aqueous solution conditions. Prog Nucl Ene.94:93-100, https://doi.org/10.1016/j.pnucene.2016.10.005.

30. Van der Bruggena B, Manttari M, Nystrom M (2008) Drawbacks of applying nanofiltration and how to avoid them: a review. Sep Purif Technol. 63:251-263, https://doi.org/10.1016/j.cej.2018.05.017.

31. Alaei MA, Hosseini SS, Ruan G, Tan NR (2015) Tailoring PES Nanofiltration Membranes through Systematic Investigations on the Effect of Prominent Design, Fabrication and Operational Parameters. RSC Adv. 5:49080-49097, https://doi.org/10.1039/C5RA05985B.

32. Al-Rashdi BAM, Johnson DJ, Hilal N (2013) Removal of heavy metal ions by nanofiltration. Desalination. 315:2-17, https://doi.org/10.1016/j.desal.2012.05.022.

33. Ozaki H, Sharma K, Saktaywin W (2002) Performance of an ultra-low-pressure reverse osmosis membrane (ULPROM) for separating heavy metal: effects of interference parameters. Desalination. 144:287-294, https://doi.org/10.1016/ S0011-9164(02)00329-6.

34. Liu F, Zhang G, Meng Q, Zhang H (2008) Performance of Nanofiltration and Reverse Osmosis Membranes in Metal Effluent Treatment. Chinese J Chem Eng. 16:441-445, https://doi.org/10.1016/S1004-9541(08)60102-0.

35. Ghaemi N, Madaeni SS, Daraei P, Rajabi S, Alizadeh AH, Heydari R, Beyghzadeh M, Ghouzivand S (2015) Polyethersulfone membrane enhanced with iron oxide nanoparticles for copper removal from water: application of new functionalized Fe_3O_4 nanoparticles. Chem Eng J. 263:101-112, https://doi.org/10.1016/j.cej.2014.10.103.

36. Fouladgar M., Beheshti M, Sabzyan H (2015) Single and binary adsorption of nickel and copper from aqueous solutions by γ-alumina nanoparticles: equilibrium and kinetic modeling. J Mol Liq. 211:1060–1073.

37. Ellis D, Bouchard C, Lantagne G (2000) Removal of iron and manganese from groundwater by oxidation and microfiltration, Desalination. 130: 255–264, https://doi.org/10.1016/S0011-9164(00)00090-4.

38. Cote P, Mourato D, Güngerich C, Russell J, Houghton E (1998) Immersed membrane filtration for the production of drinking water: case studies, Desalination. 117:181–188, https://doi.org/10.1016/S0011-9164(98)00090-3.

39. [35] Chen WH, Hsieh YH, Wu CC, Wan MW, Futalan CM, Kan CC (2011), The on-site feasibility study of iron and manganese removal from groundwater by hollow-fiber microfiltration, J. Water Supply Res. Technol. AQUA 60:391–401, https://doi.org/10.2166/aqua.2011.067.

40. [36] Tang X, Zhu X, Huang K, Wang J, Guo Y, Xie B, Li G., Liang H (2021) Can ultrafiltration singly treat the iron- and manganese-containing groundwater? J. Hazard. Mater. 409:124983 https://doi.org/10.1016/j. jhazmat.2020.124983.

41. [37] Cheng LH, Xiong ZZ, Cai S, Li DW, Xu XH (2020) Aeration-manganese sand filter-ultrafiltration to remove iron and manganese from water: oxidation effect and fouling behavior of manganese sand coated film, J. Water Process Eng. 38:101621, https://doi.org/10.1016/j.jwpe.2020.101621.

42. [38] Haddad M, Barbeau B (2019) Hybrid hollow fiber nanofiltration–calcite contactor: a novel point-of-entry treatment for removal of dissolved Mn, Fe, NOM and hardness from domestic groundwater supplies, Membranes (Basel) 9:1–13, https://doi.org/10.3390/membranes9070090.

54

J. Water Environ. Nanotechnol., 9(1): 44-54 Winter 2024